Reprogramming Fibroblasts into Bipotential Hepatic Stem Cells by Defined Factors

Bing Yu,[1,2,11] Zhi-Ying He,[1,2,11] Pu You,[1,2,10] Qing-Wang Han,[1,2] Dao Xiang,[1,2] Fei Chen,[1,2] Min-Jun Wang,[1,2]
Chang-Cheng Liu,[1,2] Xi-Wen Lin,[3] Uyunbilig Borjigin,[4] Xiao-Yuan Zi,[1,2] Jian-Xiu Li,[1,2] Hai-Ying Zhu,[1,2] Wen-Lin Li,[1,2]
Chun-Sheng Han,[3] Kirk J. Wangensteen,[5] Yufang Shi,[6,7] Li-Jian Hui,[8] Xin Wang,[4,8,9,*] and Yi-Ping Hu[1,2,*]

[1]Department of Cell Biology
[2]Center for Stem Cell and Medicine, The Graduate School
Second Military Medical University, Shanghai 200433, China
[3]State Key Laboratory of Reproductive Biology, Institute of Zoology, Chinese Academy of Sciences, Beijing 100101, China
[4]The Key Laboratory of National Education Ministry for Mammalian Reproductive Biology and Biotechnology, Inner Mongolia University,
Huhhot 010070, China
[5]Department of Medicine, Division of Gastroenterology, University of Pennsylvania, Philadelphia, PA 19104, USA
[6]Key Laboratory of Stem Cell Biology, Institute of Health Sciences, Shanghai Institutes for Biological Sciences, Chinese Academy of
Sciences/Shanghai Jiao Tong University School of Medicine, Shanghai 200025, China
[7]Child Health Institute of New Jersey and Department of Pharmacology, Robert Wood Johnson Medical School, University of Medicine
and Dentistry of New Jersey, 89 French Street, New Brunswick, NJ 08901, USA
[8]Laboratory of Molecular Cell Biology, Institute of Biochemistry and Cell Biology, Shanghai Institute for Biological Sciences, Chinese
Academy of Sciences, Shanghai 200031, China
[9]Department of Laboratory Medicine and Pathology, University of Minnesota, Minneapolis, MN 55455, USA
[10]Present address: Naval Medical Research Institute, Shanghai 200433, China
[11]These authors contributed equally to this work
*Correspondence: wangxin_cn@imu.edu.cn (X.W.), yphu@smmu.edu.cn (Y.-P.H.)
http://dx.doi.org/10.1016/j.stem.2013.06.017

SUMMARY

Recent studies have demonstrated direct reprogramming of fibroblasts into a range of somatic cell types, but to date stem or progenitor cells have only been reprogrammed for the blood and neuronal lineages. We previously reported generation of induced hepatocyte-like (iHep) cells by transduction of *Gata4*, *Hnf1α*, and *Foxa3* in *p19* Arf null mouse embryonic fibroblasts (MEFs). Here, we show that *Hnf1β* and *Foxa3*, liver organogenesis transcription factors, are sufficient to reprogram MEFs into induced hepatic stem cells (iHepSCs). iHepSCs can be stably expanded in vitro and possess the potential of bidirectional differentiation into both hepatocytic and cholangiocytic lineages. In the injured liver of fumarylacetoacetate hydrolase (*Fah*)-deficient mice, repopulating iHepSCs become hepatocyte-like cells. They also engraft as cholangiocytes into bile ducts of mice with DDC-induced bile ductular injury. Lineage conversion into bipotential expandable iHepSCs provides a strategy to enable efficient derivation of both hepatocytes and cholangiocytes for use in disease modeling and tissue engineering.

INTRODUCTION

Transcription factors are well known to modulate cell fate. It was first reported that *MyoD*, a critical transcription factor for specification of the skeletal muscle lineage during early development, could induce muscle-specific properties in fibroblasts (Davis et al., 1987). After the recent discovery that fibroblasts were reprogrammed into induced pluripotent stem cells (iPSCs) by defined transcription factors (Takahashi and Yamanaka, 2006), other particular sets of transcription factors were found for their capacities to induce several specific somatic cell phenotypes, such as hematopoietic cells (Laiosa et al., 2006; Feng et al., 2008), neuronal cells (Vierbuchen et al., 2010; Pang et al., 2011; Caiazzo et al., 2011; Pfisterer et al., 2011; Son et al., 2011; Liu et al., 2012), cardiomyocytes (Ieda et al., 2010; Efe et al., 2011), and hepatocytes (Huang et al., 2011; Sekiya and Suzuki, 2011). The direct induction of particular somatic cells from other somatic lineages enabled more efficiency and safety when compared with the early methods of staged differentiations starting from pluripotent stem cells, either embryonic stem cells (ESCs) or iPSCs.

Our recent study, as well as the work of others, indicated that mouse fibroblasts could be reprogrammed directly into induced hepatocyte-like (iHep) cells (Huang et al., 2011; Sekiya and Suzuki, 2011). iHep cells were obtained through enforced expression of three defined factors, *Gata4*, *Hnf1α*, and *Foxa3*, with controlling the senescence pathway by *p19* knockdown or knockout (Huang et al., 2011) or that of two defined factors comprising *Hnf4α* plus *Foxa1*, *Foxa2*, or *Foxa3* (Sekiya and Suzuki, 2011). In the meanwhile, we were interested in deriving several other types of liver cells, including cholangiocytes and hepatic stem cells (HepSCs), because the liver is composed of various cell types and a spectrum of liver cells will be required for both cell replacement therapies and constructing liver tissues by bioengineering. The direct induction of HepSCs caters to our

strategy of obtaining both hepatocytes and cholangiocytes. HepSCs in both embryonic and adult livers were known to be capable of self-renewal as well as differentiation into both hepatocytes and cholangiocytes. HepSCs participated in both embryonic liver organogenesis (Nejak-Bowen and Monga, 2008) and the maintenance of liver tissue homeostasis after chronic injuries (Ishikawa et al., 2012) and were used as donor cells for liver transplantation therapy (Wang et al., 2003b; Oertel et al., 2008). The successful induction of HepSCs will facilitate the study on the mechanism of hepatic transdifferentiation and the derivation of other endodermal cell types, such as insulin-secreting pancreatic beta cells for diabetic patients. Most recently, new findings about induction of tissue-specific stem cells directly from fibroblasts, including blood progenitor cells (Szabo et al., 2010) and neural stem cells (Kim et al., 2011; Lujan et al., 2012; Han et al., 2012; Thier et al., 2012; Ring et al., 2012), were reported. The new strategies in these studies were to directly reprogram fibroblasts into the desired tissue-specific stem cells through the adjustments of culture conditions suitable for the stem cells during the reprogramming process (Kim et al., 2011), as well as through modulation of defined transcription factors under specific growth conditions (Szabo et al., 2010; Lujan et al., 2012; Han et al., 2012; Thier et al., 2012; Ring et al., 2012).

Here, we report that the induced hepatic stem cells (iHepSCs) can be directly induced from mouse embryonic fibroblasts (MEFs) by overexpressing two key transcription factors, *Hnf1β* and *Foxa3*, which were originally identified during liver organogenesis (Coffinier et al., 2002; Lokmane et al., 2008; Le Lay and Kaestner, 2010). We prove that the derived iHepSCs, similar to hepatic stem cells, possess the capacities of both self-renewal and bipotency of differentiation into both hepatocytes and cholangiocytes under in vitro and in vivo conditions. iHepSCs are stable and expandable, which holds great promise for cell replacement therapy and liver tissue engineering.

RESULTS

Directly Inducing MEFs into iHepSCs by *Hnf1β* and *Foxa3*

Our procedure from initial transcription factor screening to in vitro and in vivo characterization of iHepSCs is summarized in a diagram (Figure 1A). A total of 20 candidate factors, which were known to have critical roles either for embryonic liver organogenesis (Zaret and Grompe, 2008; Le Lay and Kaestner, 2010; Zaret, 2008) or for activation of oval cells in adult mouse livers (Jakubowski et al., 2005), were selected to test their potential capacity for inducing iHepSCs from MEFs (Table S1 available online). Similar with previous reports (Zaret, 2008; Okabe et al., 2009), expression of markers for hepatic stem cells, including *EpCAM*, alpha-fetoprotein (*Afp*), albumin (*Alb*), and transthyretin (*Ttr*), was used to determine the phenotype of iHepSCs. Candidate factors were cotransfected into MEFs to determine the minimum factors required to convert MEFs into iHepSCs. Among all factors screened, *Hnf1β* and *Foxa3* were proven to be sufficient for this conversion. The screening results are summarized in Figures S1A–S1C.

Epithelial cell clusters that emerged from the MEFs were found at 15 days after transfection with both *Hnf1β* and *Foxa3* at a frequency of morphological conversion of 0.4% ± 0.082%

(Figure 1B and Figure S1D), whereas no such conversion appeared with an eGFP-control lentivirus (data not shown). Newly induced epithelial cells were enriched and collected for analysis. Converted cells had the typical morphological phenotypes of epithelial cells (Figures 1C and 1D). RT-PCR analysis revealed that these converted epithelial cells expressed markers of hepatocytes (*Alb*, *Ttr*, and *Hnf4α*), of cholangiocytes (*CK19*), and of both hepatocytes and cholangiocytes (*CK8* and *CK18*) (Figure 1E). In addition, the converted epithelial cells also expressed markers of hepatic stem cells (*Afp*, *Sox9*, *EpCAM*, and *Dlk1*) (Figure 1E). In contrast, they did not express the genes of mature hepatocytes in adult liver (*G6p*, *Tat*, *Cyp3a11*, and *Cyp7a1*) (Figure 1E). Thus, these cells were further characterized to test whether they are iHepSCs by using several assays in vitro and in vivo.

We proved that the possibility of contamination of cells from other early enteric organ systems was excluded. Head and visceral tissues in the embryos were completely removed during tissue harvesting. Especially, we confirmed that both MEFs and MEF-derived iHepSCs did not express pancreatic lineage markers (*Pdx1*, *Ins1*, *Amylase*, and *Glucagon*) or intestinal lineage cell markers (*Secretin*, *Cdx1*, *Lysozyme*, and *Chromogramin A*) (Figure S1E). Therefore, iHepSCs were only converted from fibroblasts but not from the embryonic cells of any other organs such as the pancreas and intestine.

Additionally, we also used tail tip fibroblasts (TTFs) of adult mice to induce iHepSCs under the same conditions. Fifteen days after transfection with *Hnf1β* and *Foxa3*, the epithelial clones, morphologically similar as MEF-derived iHepSCs, were observed in the TTF culture (Figure S1F). Similar to MEF-derived iHepSCs, the TTF-derived epithelial cells expressed hepatic and biliary markers (*Alb*, *Ttr*, *Afp*, *CK8*, and *CK18*) and some hepatic stem cell markers (*Dlk1* and *EpCAM*) (Figure S1F). However, the TTF-derived iHepSCs showed proliferation arrest and cell death after three to four rounds of passages (Figure S1F).

Converted Epithelial Cells Possessed the Basic Characteristics of Hepatic Stem Cells

Ten single-cell clones (clones from 1 to 10) were selected from the pool of two-factor converted epithelial cells for additional investigation of hepatic stem cell properties in vitro. Overall, the converted epithelial cells of these selected colonies showed similar mRNA expression pattern (Table S2). In parallel analyses, cells of clones 2 and 6 were studied for general features of hepatic stem cells and bipotential hepatic differentiation. First, self-renewal capacity was evaluated. The iHepSCs displayed a typical S-shaped growth curve and the mean population doubling time was approximately 20 hr, while the doubling time of MEFs (passage 4) was 36 hr (Figures 1F and 1G). There was little difference in doubling time or shape of growth curve at passage 10 and passage 30, suggesting that iHepSCs retained stable self-renewal capacity after multiple cell divisions in vitro. Second, cells of two selected colonies kept normal diploid nuclear DNA levels on fluorescence-activated cell sorting analysis (Figure S2A). Furthermore, iHepSCs in clone 2 and clone 6 kept normal karyotypes up to passage 32 (Figure S2C).

The converted epithelial cells were positive for E-cadherin (Figure 2A) and negative for α-SMA (data not shown), which proves that they completed mesenchymal-epithelial transition
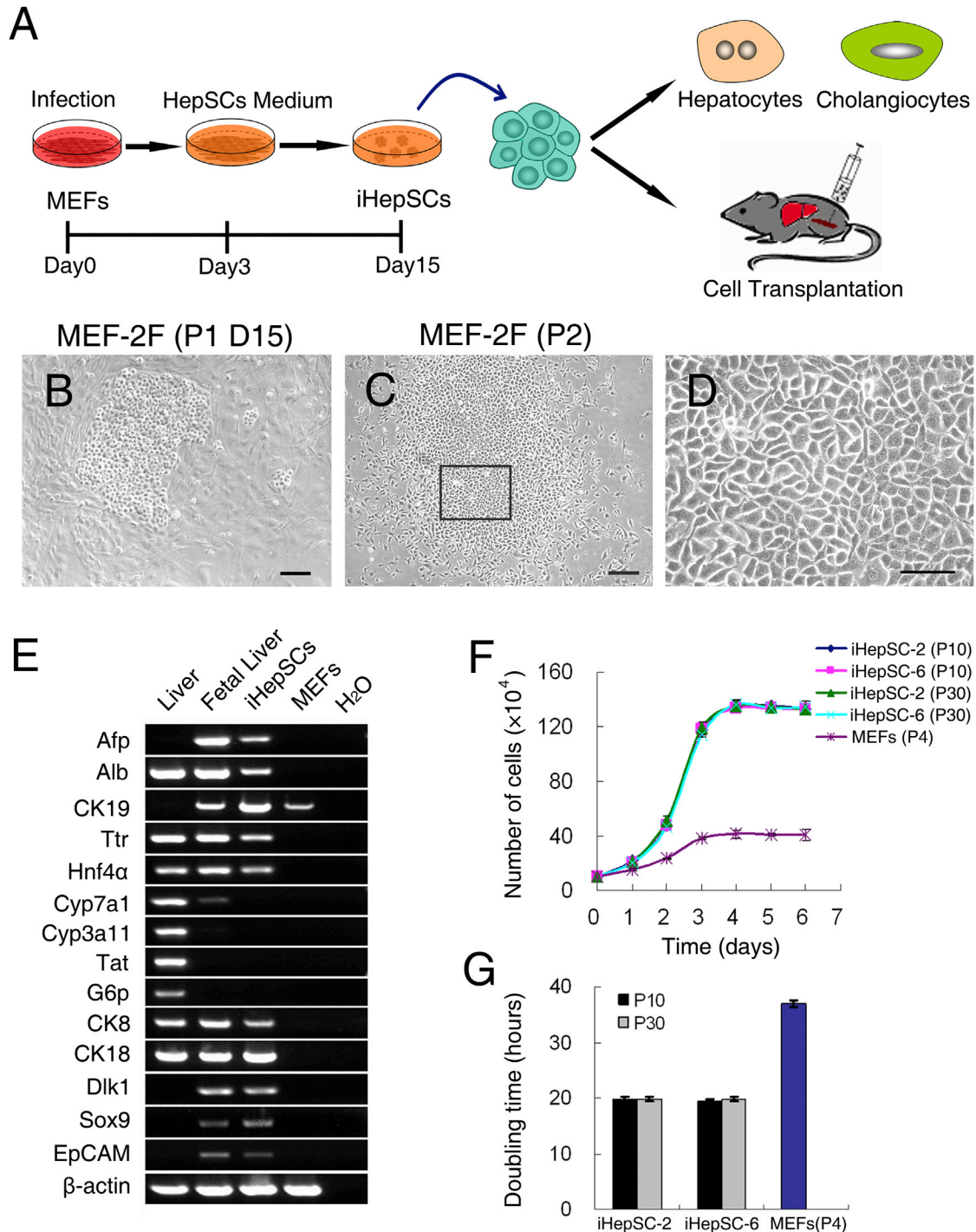
Figure 1. Conversion of MEFs into iHepSCs by *Hnf1β* and *Foxa3*

(A) Schema of the experimental procedures including direct induction of iHepSCs by defined factors, in vitro differentiations, and in vivo cell transplantation assays.

(B) Representative epithelial clone emerged from the MEFs at 15 days postinfection with *Hnf1β* and *Foxa3* (passage 1).

(C and D) The same epithelial clone shown after expansion (passage 2) (C), and the outlined area in (C) was magnified to show converted morphology of epithelial cells in the clone (D).

(E) RT-PCR results for detection of hepatic gene expressions in the converted epithelial cells, adult liver cells, fetal liver cells, and MEFs were used as controls.

(F and G) Growth curves (F) and cell doubling times (G) for two iHepSC clones, iHepSC-2 and iHepSC-6 (both passage of 10 and passage of 30), in comparison with MEFs (passage 4). Data represent mean ± SD (n = 3). P, passage number; D, days after passage of cells. Scale bar represents 100 μm.

See also Figure S1 and Table S1.

(MET) from fibroblasts. Similar to previously reported hepatic stem cells, the iHepSCs expressed markers of embryonic hepatic progenitors (Alb, Afp, and CK19) (Figures 2D and 2E) and markers of hepatic stem cells (EpCAM, Pan-CK, Sox9, and Lgr5) (Figures 2B, 2C, 2F, and 2G) (Furuyama et al., 2011; Huch, et al., 2013). Ultrastructural analysis was performed with electron microscopy, which showed that the iHepSCs had a high nuclear-to-cytoplasm ratio and few cytoplasmic organelles, which are characteristics of stem cells (Figure S2B). These results suggested that the converted epithelial cells possessed the general features of hepatic stem cells.

To further evaluate the overall reprogramming status of the converted epithelial cells, their global gene expression profiles were compared with those of several other types of cells, including: (1) liver epithelial progenitor cells (LEPCs), defined hepatic stem cells from our previous study (Li et al., 2006); (2) our previously reported induced adult hepatocyte-like (iHep) cells (Huang et al., 2011); (3) primary adult hepatocytes prepared from mouse liver; and (4) MEFs as the control of original cells before induction of cell conversion. The induced cells clustered closely with LEPCs but separated from MEFs, iHep cells, and mature hepatocytes (Figure 2H). Indeed, the gene expression patterns of induced cells were similar with LEPCs in gene categories of liver development, stem cell signal pathways, fat metabolic pathways, and glucose metabolic pathways, although there were some minor differences in gene expression profiles between iHepSCs and LEPCs (Figure S2D). Furthermore, we compared the global gene expression of iHepSCs with three recently published adult liver stem or progenitor cells (Shin et al., 2011; Dorrell et al., 2011; Huch et al., 2013). iHepSCs were most similar to sorted M$^+$133$^+$26$^-$ liver progenitor cells and Foxl1$^+$ liver progenitor cells and to a lesser extent to Lgr5$^+$ liver stem cells, indicating that the iHepSCs bear true similarity to naturally existing liver stem or progenitor cells (Figure S2E). All together, these results suggested that the induced epithelial cells had significant similarity with adult liver stem cells but were different than mature hepatocytes and MEFs. These results strongly supported the conclusion that *Hnf1β* and *Foxa3* were able to induce MEFs into iHepSCs.

The Bipotency of iHepSCs Differentiated into Both Hepatocytes and Cholangiocytes

We next investigated whether the iHepSCs possessed the bipotency of hepatic stem cells to differentiate into both hepatocytic and cholangiocytic lineages in vitro. To prove that iHepSCs could be induced for hepatocytic differentiation, we plated the iHepSCs on Matrigel in hepatic differentiation medium (HDM) with oncostatin M (OSM) and epidermal growth factor (EGF). After 24 hr, the plated cells formed aggregates on the surface of the Matrigel. The aggregates had smooth edges and reached up to approximately 100 μm in diameter in size by day 6 after plating (Figure 3A). Beyond 6 days after plating, the rate of proliferation of the cell aggregates gradually slowed down and stopped at around 12 days. Several assays were performed to prove that the differentiated cells from iHepSCs in the aggregates became mature hepatocytes. PAS staining of frozen sections of the iHepSCs-derived cells showed significant glycogen storage as mature hepatic cells (Figure 3B). Similarly, chiquoine staining indicated glucose-6-phosphatase (G6P) activity (Fig-

ure 3C). The efficiency of hepatic differentiation was determined by quantifying the percentage of albumin-positive and CK19-negative cells in the aggregates. The rate of differentiation into hepatocyte-like cells of iHepSCs was 56.4% ± 14.7% (Figures 3D–3F). RT-PCR analysis revealed robust upregulation of mature hepatocyte-specific transcripts (*Alb*, *Hnf4α*, *Aat*, *Gjb1*, *Cyp3a11*, *Cyp7a1*, and *G6p*) in the cells at 12 days after hepatic differentiation. Meanwhile, the markers of cholangiocytes (gamma-glutamyl transpeptidase, *Ggt*) and of fetal liver progenitor cells (*Dlk1*) were not detectable in the same cells (Figure 3I). Additionally, ultrastructural analysis with electron microscopy showed typical hepatocytic organelles such as mitochondria, lysosomes, and glycogen granules (Figures 3G and 3H). Furthermore, many bile canaliculi were observed in the intercellular space of adjacent cells (Figure 3H). Using ELISA, we found significant Alb secretion into the medium by the induced cell aggregates (Figure 3J, p < 0.05). All together, these results clearly indicated that iHepSCs could differentiate into hepatocyte-like cells.

When iHepSCs were cultured in a three-dimensional (3D) type I collagen gel culture system (Li et al., 2010), they differentiated into cholangiocyte-like cells with representative branching structures and expressed cholangiocyte marker CK19 after 9 days of induction (Figure 4A). Many iHepSC-derived cells in the branching structures showed alkaline phosphatase activity, indicating a functional phosphatase specifically expressed in iHepSC-derived cholangiocyte-like cells (Figure 4B). Ultrastructural analysis with electron microscopy showed basement membrane on one side and microvilli on the opposite side in the induced cells, which are typical features of cholangiocytes (Figures 4D and 4E). Additionally, we compared the gene expression profiles between iHepSC-derived cholangiocytes and primary cholangiocytes (Shin et al., 2011). The gene expression profiles of iHepSC-derived cholangiocytes clustered with that of primary cholangiocytes, indicating successful cholangiocytic differentiation of iHepSCs in vitro (Figure 4C). To further evaluate the function of iHepSC-derived cholangiocytes, we induced iHepSCs to form cysts in the 3D culture system containing 1.2 mg/ml type I collagen and 40% Matrigel (Tanimizu et al., 2007). About 10% of iHepSCs-derived cells were found in round cysts of monolayer of cells after 7 days of induction (Figure 4F), while the other iHepSC-derived cells formed branching structures. The iHepSC-derived cholangiocyte-like cells in cysts expressed the two conventional cholangiocyte markers, CK19 (Figures 4I and 4K) and CK7 (Figures 4L and 4N). The induced cholangiocyte-like cells in cysts showed apicobasal polarity as with primary cholangiocytes. They had F-actin localized to the inner layer of the lumen (Figures 4J, 4K, 4M, and 4N). Remarkably, the cholangiocyte-like cells in cysts showed secretory function as primary cholangiocytes. The cholangiocyte-like cells in cysts transported Rhodamine 123 into the cyst lumen (Figure 4G). Their transport function was blocked in the presence of the MDR inhibitor Verapamil (Figure 4H). Collectively, these findings supported that iHepSCs had differentiated into cholaniocyte-like cells.

iHepSCs Differentiated into Both Hepatocytes and Cholangiocytes In Vivo

Fumarylacetoacetate hydrolase-deficient (*Fah*$^{-/-}$) mice defective in tyrosine metabolism require a supply of 2-(2-nitro-4-trifluoromethylbenzoyl)-1, 3-cyclohexanedione (NTBC) for
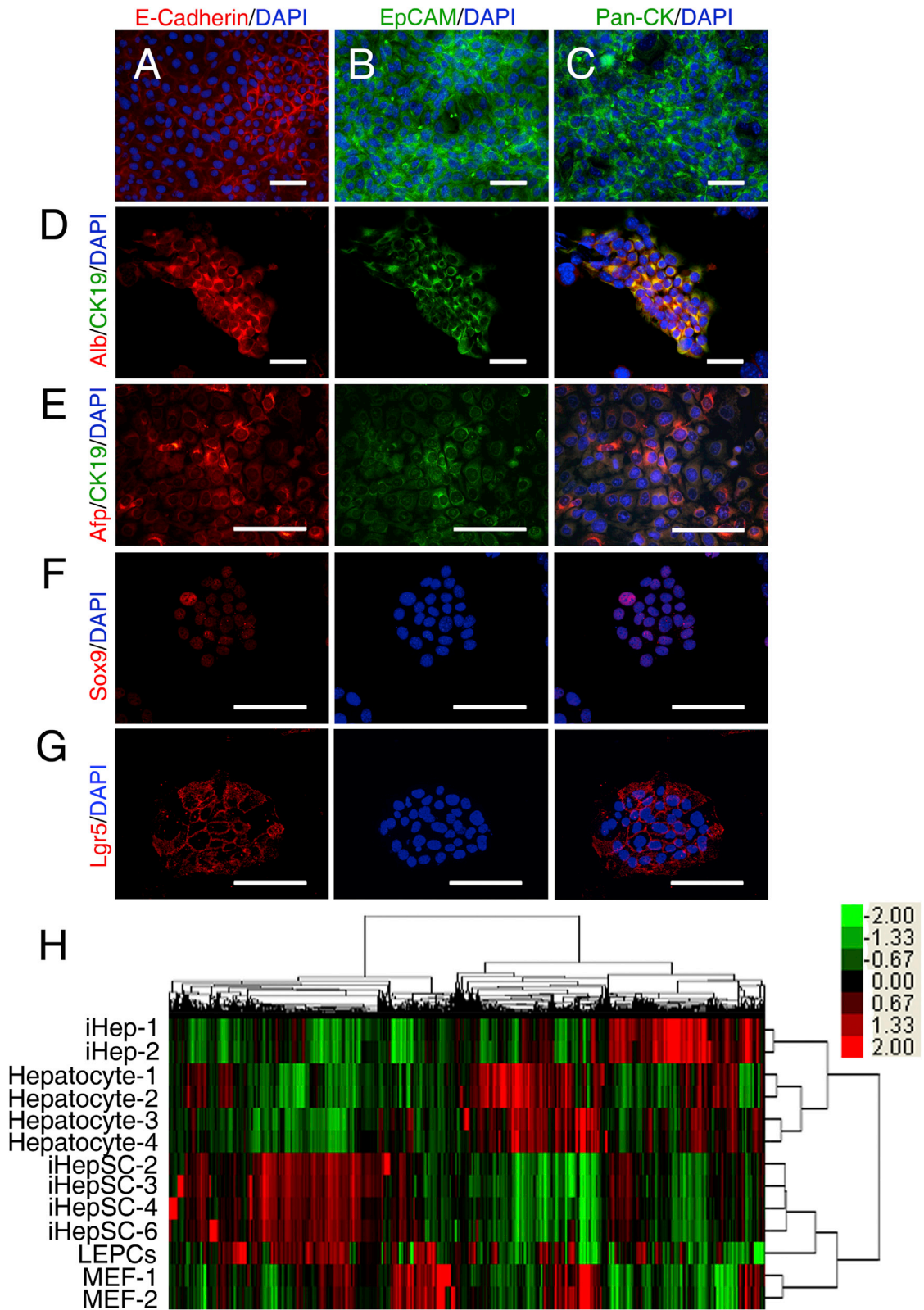
survival. If NTBC is withdrawn, they undergo liver failure and death. $Fah^{-/-}$ mice can be rescued by transplantation of wild-type hepatocytes after NTBC withdrawal (Grompe et al., 1993; Overturf et al., 1996; Wang et al., 2003a), representing a robust model to characterize in vivo repopulation. Here, $Fah^{-/-}$ mice were used to prove the in vivo differentiation of functional hepatocytes from iHepSCs. We intrasplenically injected iHepSCs into $Fah^{-/-}$ mice, while wild-type hepatocytes and MEFs were used as the controls. All six of $Fah^{-/-}$ mice transplanted with MEFs died within 6 weeks. In contrast, four out of 11 $Fah^{-/-}$ mice transplanted with iHepSCs survived 8 weeks without NTBC (Figure 5A). Analysis of liver samples from these recipients indicated that Fah-positive cells derived from iHepSCs comprised 11.6% ± 3.6% (7.9% to 16.2%) of total hepatocytes in liver of $Fah^{-/-}$ mice (Figure 5B). This level of liver repopulation was similar to that in $Fah^{-/-}$ mice transplanted with hepatic progenitor cells (Li et al., 2010; He et al., 2010, 2012). Morphologically, Fah-positive nodules showed normal liver sinusoid structures. Some Fah-positive hepatocytes were binucleated, similar to wild-type hepatocytes (Figure 5C). In contrast, recipients transplanted with MEFs had no repopulation from Fah-positive hepatocytes. Analysis of liver samples revealed that all of the endogenous hepatocytes were Fah negative with disrupted cellular structures (data not shown). Remarkably, repopulated Fah-positive hepatocytes from iHepSCs were also found to express Alb by immunofluorescence (Figure 5D). Repopulating Fah-positive cells were harvested by laser-capture microdissection and were found to have gene expression patterns that were the same as those of host hepatocytes but different than those of iHepSCs without differentiation (Figures S3A and S3B). Moreover, $Fah^{-/-}$ mice transplanted with iHepSCs had restoration of liver function, as evidenced by a significantly corrected level of serum albumin when compared with controls. Recipients of iHepSCs also had lower levels of aspartate aminotransferase (AST), alanine transaminase (ALT), and total bilirubin compared with controls, indicating that transplantation of iHepSCs attenuated liver injury (Figure 5E). Together, these results demonstrated that iHepSC-derived hepatocytes were able to engraft into the liver of $Fah^{-/-}$ mice as normal hepatocytes.

The 3,5-diethoxycarbonyl-1,4-dihydrocollidine (DDC)-fed mouse is a well-known model for liver progenitor cell (oval cell) activation and bile ductular proliferation (Preisegger et al., 1999). In vivo DDC treatment induces oval cells to spontaneously differentiate into cholangiocytes (Preisegger et al., 1999; Sackett, et al., 2009; Thompson et al., 2010). We used DDC-fed mice to determine whether iHepSCs possess the ability to engraft into bile ducts and further differentiate into cholangiocytes in vivo. After transfection with eGFP-expressing lentivirus, 1×10^6 iHepSCs were transplanted into 15 DDC-treated mice. eGFP-positive cells were found scattered within large bile ducts in the livers of four recipient mice 3 weeks post-

transplantation and comprised 1.44% ± 0.41% of total biliary epithelial cells (Figures 6A and 6B). eGFP-positive cells expressed CK19, EpCAM, and CK7, markers of biliary epithelial cells (Figure 6C, 6D, and 6E). In addition, eGFP-positive cells also expressed Ostα (Figure 6F), which is a major bile acid and steroid transporter and is a functional marker of cholangiocytes (Ballatori et al., 2005). Furthermore, a second cell marker was used to identify transplanted cells. After iHepSCs were transfected with LacZ-expressing lentivirus, LacZ-positive cells were also found to be scattered within large bile ducts in the liver of recipient mice 3 weeks posttransplantation (Figures S4A, S4B, and S4D). The LacZ-positive cells costained with CK19, further confirming that iHepSCs could differentiate into cholangiocytes in vivo (Figures S4C, S4E, and S4F). Importantly, the possibility of cell fusion between iHepSC-derived cells and cells of host liver was excluded by using a floxed-lacZ reporter mouse model that allowed $lacZ$ gene to express only in the fused cells (Figures S4G–S4I). Collectively, these results demonstrated that iHepSCs had the capacity to differentiate into cholangiocytes in the liver of DDC-treated mice after transplantation.

It is worth mentioning that there were no tumors in any of the recipients, including $Fah^{-/-}$ mice and DDC-treated mice. In addition, there were no tumors in six NOD/SCID mice subcutaneously transplanted with 1×10^6 iHepSCs during a 12-week time frame (Figure S4J). These data indicate that iHepSCs were not contaminated with potentially tumorigenic cells. However, the longer-term risk of tumorigenesis will be examined in our future experiments.

DISCUSSION

iHepSCs would be a useful cell type for autologous cell therapy and liver tissue engineering. They would also be useful to model hepatic stem cells in drug discovery and in the analysis of the pathogenesis of human liver diseases. In comparison to previous methods of staged differentiation to derive tissue-specific somatic cells from ESCs or iPSCs, the direct induction methods described here have advantages in saving time and materials. These methods eliminate the possibility of contaminating cells types such as ESCs or iPSCs, which eliminates the possibility of teratoma formation. Studies on the direct induction of tissue-specific stem cells would also be helpful in understanding the mechanisms for differentiation of tissue-specific stem cells. To our knowledge, generation of iHepSCs is the first description of direct induction of hepatic stem cells.

Our success in generating iHepSCs was the result of using both the modulation on the expression of $Hnf1\beta$ and $Foxa3$ plus the adjustments of culturing conditions during induction and selection procedures. The cell culture conditions used for direct induction of iHepSCs, including medium selection and cell passage, were designed to be suitable for hepatic stem

---

Figure 2. Characterizations of iHepSCs

(A–C) The expressions of E-Cadherin (A), EpCAM (B), and Pan-CK (C) in iHepSCs were recognized by assay of immunostaining.

(D and E) The coexpression of Alb and CK19 (D) and Afp and CK19 (E) in the iHepSCs was found by immunostaining.

(F and G) The expression of Sox9 (F) and Lgr5 (G) in an expanding clone of iHepSCs was found by immunostaining.

(H) Hierarchial clustering analysis of global gene expression profiles to compare iHepSCs with other relative cells. Scale bar represents 100 μm.

See also Figure S2 and Table S2.
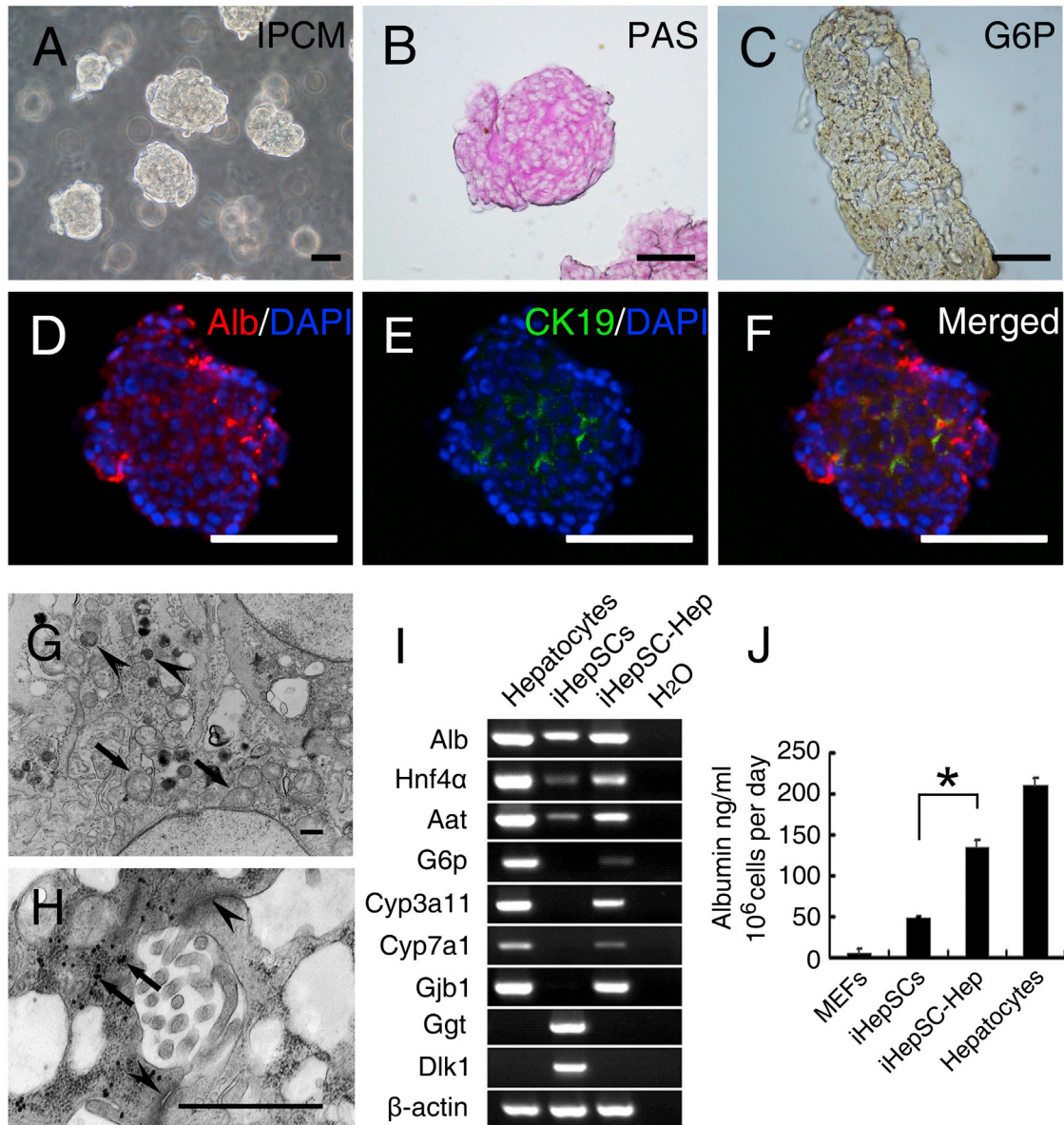
Figure 3. iHepSCs Differentiated into Mature Hepatocytes In Vitro

(A) Representative aggregates formed by iHepSCs after hepatic differentiation.

(B and C) Glycogen storage (B) and Glucose-6-phosphatase (G6p) activity (C) found in iHepSC-derived hepatic cells by assay of PAS staining and chiquoine staining, respectively.

(D–F) iHepSC-derived hepatic cells lost the expression of cholangiocyte marker CK19 (E) and only expressed Alb (D). (F) merged picture of (D) and (E).

(G and H) Ultrastructure of iHepSC-derived hepatic cells showed the morphological features of mature hepatocytes, including well-developed organelles and intercellular canaliculi. Arrowheads and arrows in (G) indicate lysosomes and mitochondria, respectively. Arrowheads and arrows in (H) indicate sites of tight junctions and glycogen granules, respectively.

(I) The comparisons among iHepSC-derived hepatic cells (iHepSC-Heps), iHepSCs, and primary hepatocytes for the expressions of representative genes relative to both hepatocytes and cholangiocytes by RT-PCR analysis.

(J) ELISA showed the significant levels of secretory Alb by iHepSC-Hep, and the data were represented as mean ± SD (n = 3; *p < 0.05, LSD t test). Scale bar represents 100 μm in (A)–(D) and 1 μm in (E) and (F).

cell cultures based on previous reports (Tanimizu et al., 2004; Li et al., 2010), which were different from the culture conditions that we used for direct induction of iHep cells (Huang et al., 2011). How transcription factors coordinate with environmental conditions to induce iHepSCs is an area of active investigation. A total of 20 candidate factors were selected for our screen based on their roles during hepatic differentiation and liver organogenesis. We found that both *Foxa3* and *Hnf1β* were necessary for the induction of iHepSCs. *Foxa3* was known as one of the defined factors for induction of iHep cells, which are a close relative to
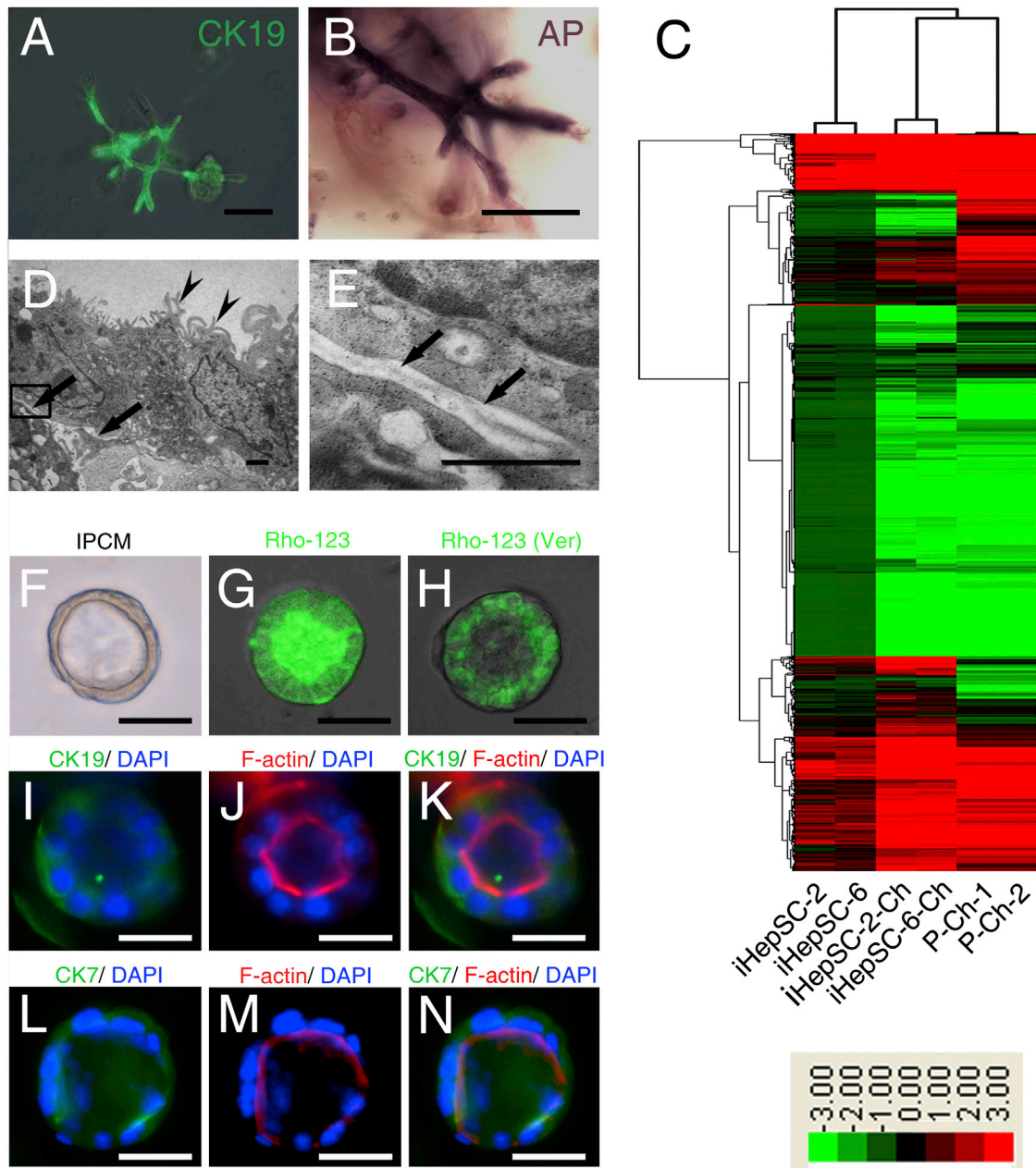
Figure 4. iHepSCs Differentiated into Cholangiocyte In Vitro

(A) CK19 immunostaining on the representative branching structures formed by the iHepSC-derived cells cultured in the 3D collagen type-1 gel.

(B) Staining for alkaline phosphase activity in the iHepSC-derived cells that formed branching structures (purplish red).

(C) Hierarchical clustering heatmap of 17,746 genes from Primary Cholangocytes (P-Ch-1 and P-Ch-2), iHepSC-derived cholangiocytes (iHepSC-2-Ch and iHepSC-6-Ch), and iHepSCs (iHepSC-2 and iHepSC-6). iHepSC-derived cholangiocytes clustered with primary cholangiocytes.

(D and E) Ultrastructure of basement membrane (arrow) and microvilli (arrowhead) of iHepSC-derived cells for detection of cholangiocytic differentiation.

(E) Magnification of the outlined area in (D) showed the details of basement membrane (arrow) with typical feature of cholangiocytes.

(F) Morphology of the iHepSC-derived ductal cysts formed in a 3D culture system.

(G) Transport of rhodamine 123 (Rho-123) into the central lumen of a cyst.

(H) The MDR inhibitor verapamil (Ver) blocks rhodamine 123 transport.

(I–K) Coimmunofluorescence staining for CK19 (I) and F-actin (J). (K) shows a merged picture of (I) and (J).

(L–N) Coimmunofluorescence staining for CK7 (L) and F-actin (M). (N) shows a merged picture of (L) and (M). Scale bar represents 100 μm in (A), (B), and (F)–(N) and 1 μm in (D) and (E).
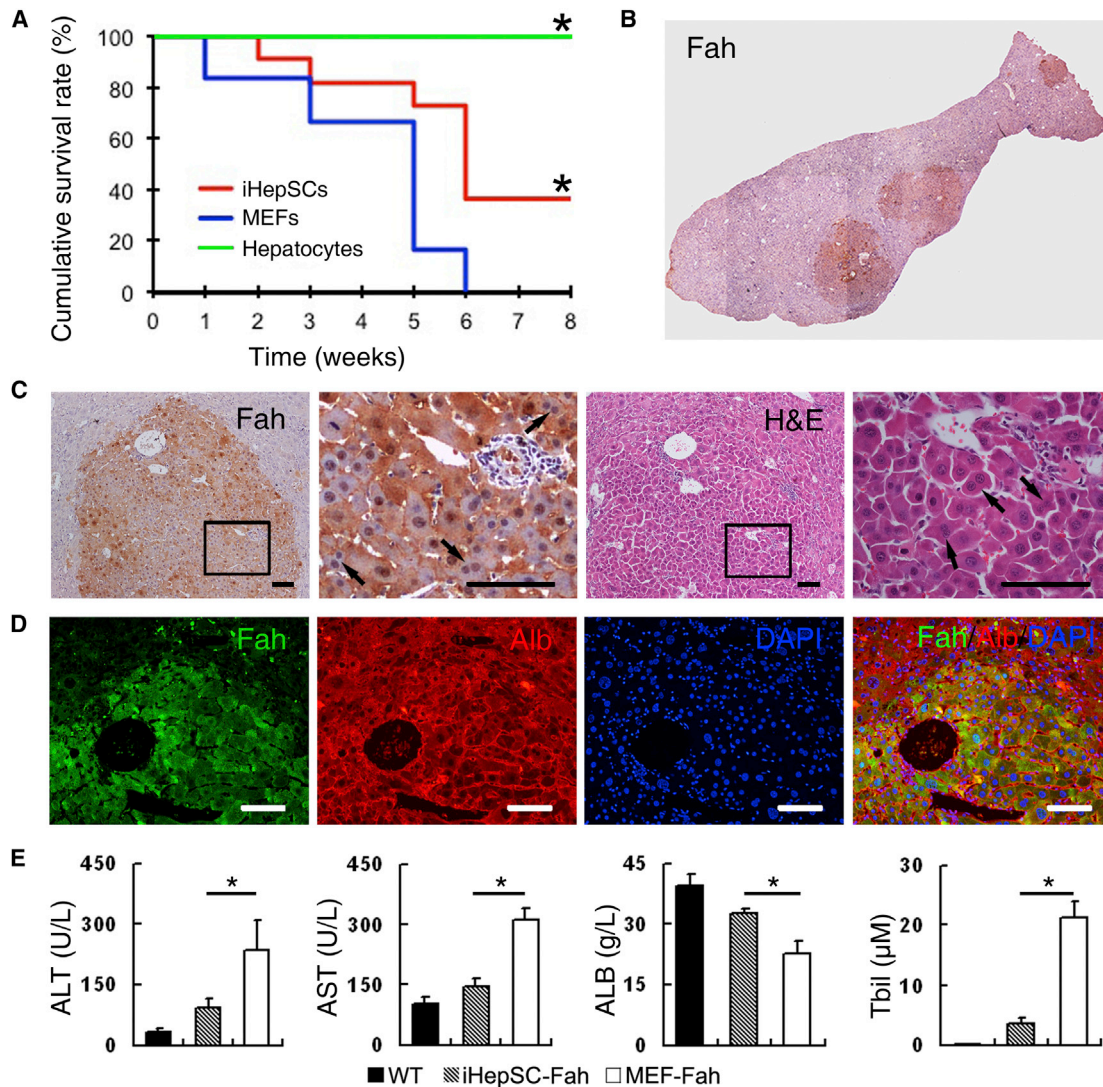
Figure 5. Engraftment of iHepSCs into the Liver Parenchyma and In Vivo Differentiation into Hepatocytes
(A) Kaplan-Meier survival curves of hepatocyte-transplanted Fah$^{-/-}$ mice (n = 6), iHepSCs-transplanted Fah$^{-/-}$ mice (n = 11), and MEFs-transplanted Fah$^{-/-}$ mice (n = 6) after NTBC withdrawal. Log rank test revealed differences between the curves for iHepSCs and MEFs (p < 0.05) and iHepSCs and hepatocytes (p < 0.05).
(B) Fah staining of repopulated iHepSCs nodules in liver sections.
(C) Histological analyses showed that the engrafted hepatocytes in livers of Fah$^{-/-}$ mice were positive for Fah protein expression and showed normal hepatocyte morphology in H&E staining. Arrows indicate binucleated hepatocytes.
(D) The repopulation nodules of iHepSC-derived hepatocytes in livers of Fah$^{-/-}$ mice recipients coexpressed Alb and Fah by immunofluoresence staining.
(E) Biochemical analysis of metabolic function of Fah$^{-/-}$ recipients. The levels of ALT, AST, ALB, and total bilirubin in WT mice (n = 4), Fah$^{-/-}$ recipients repopulated by iHepSC-derived hepatocytes (n = 4), and Fah$^{-/-}$ mice transplanted with MEFs (n = 4) are shown. The data are represented as means ± SD. *p < 0.05, LSD t test. Scale bar represents 100 μm.
See also Figure S3.

iHepSCs in the hepatic lineage. *Hnf1β*, in contrast, is unique to iHepSC derivation, and we speculate that it has a critical role in the induction of iHepSCs. Previously, *Hnf1β* was known to be required for hepatic specification of ventral endoderm and for both inducing and maintaining expression of some early hepatic transcriptional factors during liver development (Coffinier et al., 2002; Lokmane et al., 2008). Our results support a role for *Hnf1β* in directing cells reprogramming toward an early developmental stage. In addition, *Hnf1β* has been shown to be essen-tial for formation of functional bile duct system during embryogenesis (Coffinier et al., 2002; Lokmane et al., 2008). Furthermore, *Hnf1β* is strongly expressed throughout the biliary system and in periportal hepatocytes in adults (Coffinier et al., 2002). Thus, we speculate that *Hnf1β* might adjust the reprogramming direction to an earlier developmental stage that enables cholangiocyte differentiation. The results from cDNA microarray support this hypothesis because the global gene expression profiles of iHepSCs clustered with those of our previously
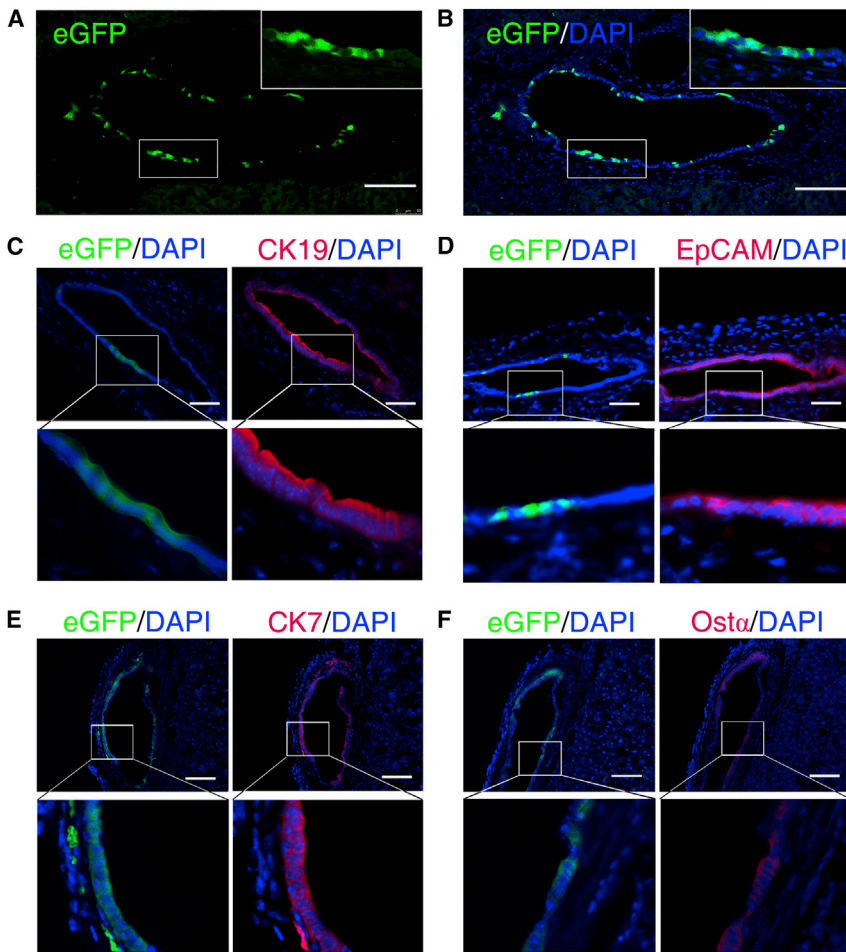
Figure 6. Engraftment of iHepSCs into the Bile Ducts and In Vivo Differentiation into Cholangiocytes

(A) Discontinuous distribution of iHepSC-derived cells labeled by eGFP in the large bile ducts of livers in DDC-treated mice after transplantation.

(B) Nuclei in (A) were counterstained with DAPI.

(C) The eGFP-positive iHepSC-derived cells found in large bile ducts expressed cholangiocyte marker CK19 by immunofluoresence staining.

(D and E) The eGFP-positive iHepSC-derived cells found in large bile ducts expressed cholangiocyte marker EpCAM (D) and CK7 (E) by immunofluoresence staining.

(F) The eGFP-positive iHepSC-derived cells found in large bile ducts expressed cholangiocyte functional marker Ostα expression by immunofluoresence staining. Scale bar represents 100 μm. See also Figure S4.

arrest that we observed with TTFs during induction of iHepSCs. The modification of other induction conditions, such as to use small molecular inducers and to readjust the reprogramming of cells at a common intermediate stage (Kim et al., 2011) will also be investigated in future work.

Up to now, there was no report of successful in vivo bile duct cell repopulation in bile duct structures. We tested iHepSCs in several reported model systems including mice with two-thirds partial hepatectomy (Oertel et al., 2008), retrorsine treatment (Li et al., 2006), experimental cholestasis using the α-naphthylisothiocyanate (ANIT)-based diet (Moritoki et al., 2006), and DDC treatment (Wang et al., 2003b). Among all of the tested models, donor iHepSC-derived cells that were positive for CK19 expression were found only in retrorsine and DDC-treated mice. However, only a few iHepSC-derived cholangiocytes positive for CK19 expression were found in retrorsine-treated mice, although a significant number of iHepSC-derived hepatocytes could be found (data not shown). In addition, iHepSC-derived cholangiocytes positive for CK19 expression were not in duct structures. Theoretically, retrorsine-treated mice are useful to assay for hepatocytes, although small numbers of engrafted cholangiocytes derived from transplanted fetal liver progenitor cells have been observed (Shafritz and Dabeva, 2002). In contrast, the DDC-treated mouse model was found to be very suitable for investigation of engraftment into the bile ducts of iHepSC-derived cholangiocytes. Our results suggest that the DDC-treated mouse model is ideal for transplantation assays of any stem cell-derived cholangiocytes.

reported liver progenitor cell lines (LEPCs) and with three recently published adult liver stem or progenitor cells (Shin et al., 2011; Dorrell et al., 2011; Huch et al., 2013) but were separate from iHep cells, mature hepatocytes, and MEFs. The induction of iHepSCs is not successful if either *Foxa3* or *Hnf1β* is left out or if any of the culture conditions are changed. Interestingly, *Jun* can be added to enhance this process but is not required for the final induction results.

Besides using MEFs, we have also tested tail tip fibroblasts (TTFs) of adult mouse for generation of iHepSCs under the same conditions. Although the expected reprogramming happened partially in TTF-derived cells, which showed iHepSC-like morphology, the gene expression profiles did not reach that of hepatic stem cells. In contrast to MEF-derived iHepSCs, these TTF-derived cells were not able to expand in vitro. These results suggest that some unidentified factors, other than our 20 candidates, are required to achieve the complete conversion from adult fibroblasts to iHepSCs. Indeed, MEFs have more plasticity when compared with TTFs (Park et al., 2008; Pang et al., 2011). On the other hand, our previous study for induction of iHep cells indicated that blockage of liver cell senescence by using *p19* null mice was necessary to overcome the proliferative hurdle of transdifferentiation (Huang et al., 2011). It is possible that TTFs are more prone to undergo senescence than MEFs during induction of iHepSCs, which might explain the proliferation

In summary, mouse embryonic fibroblasts were directly transdifferentiated into induced liver stem cells (iHepSCs) by expressing *Hnf1β* and *Foxa3*. iHepSCs not only show morphologic characteristics of liver stem cells but also possess many characteristics of liver stem cells in self-renewal and gene expression profiles. More importantly, we prove that iHepSCs have

bidirectional differentiation potential to both hepatocytic and cholangiocytic lineages in in vitro and in vivo studies.

EXPERIMENTAL PROCEDURES

Cell Culture and Generation of iHepSCs

MEFs (1×10^5, Passage 4) were seeded on gelatin-coated 35 mm dishes and infected with lentivirus-expressing transcription factors the next day. After 3 days infection, the MEF medium was replaced by the HepSCs medium (Dulbecco's modified Eagle's medium [DMEM]/F12 medium supplemented with 10% fetal bovine serum [HyClone], 1% penicillin/streptomycin, 0.1 mmol/l 2-mercaptoethanol [both from GIBCO-BRL], 10 ng/ml HGF, 10 ng/ml EGF [both from R&D Systems], $1 \times$ insulin-transferrin-selenium [ITS], 10^{-7} mol/l dexamethasone, 10 ng/ml nicotinamide, and 50 mg/ml gentamicin [all from Sigma-Aldrich]) suitable for hepatic stem cell induction, maintenance, and proliferation (Tanimizu et al., 2004; Li et al., 2010). Fifteen days later, the cells were treated with 0.05% Trypsin/EDTA for 2 min to discard the detached fibroblast cells and the remaining epithelial cells were enriched. Then the induced epithelial cells (1×10^5) were plated on gelatin-coated 60 mm dish and were incubated in HepSC medium for 8 days. Single epithelial colonies were picked, expanded, and characterized by proliferation assays, karyotype analysis, RT-PCR analysis, immunochemistry, and microarray analysis as given in the Supplemental Information.

In Vitro Differentiation

For the generation of hepatocytes, the method of iHepSC hepatic differentiation was modified from our previous procedure (Li et al., 2006). Matrigel (BD Biosciences) was poured into 6-well Ultra Low Cluster Plates (Corning Costar) and then was placed at 37°C for 30 min to form the gel. Cells of clone 2 or 6 (1×10^5) were suspended in hepatic differentiation medium (HDM) (DMEM/F12 medium supplemented with 10% fetal bovine serum [HyClone], 20 ng/ml Oncostatin M, 20 ng/ml EGF [both from R&D], 10 ng/ml nicotinamide, 0.1 mmol/l L-Ascorbic acid and 10^{-7} mol/l dexamethasone [all from Sigma-Aldrich]). The culture medium was changed every 2 days. After 12 days, the induced cells were harvested from the top of matrigel gel by dispase and then were used for RNA preparation, periodic acid Schiff (PAS) staining, chiquoine staining, and ultra structure analysis, as previously described in Huang et al. (2011) and Li et al. (2006).

For the generation of cholangiocytes, three-dimensional culture system using collagen type1 (BD) was used according to the manufacture's instruction. In brief, 800 μl Collagen type1, 100 μl 10× PBS, 20 μl 1N NaOH, and 80 μl H$_2$O were mixed on ice. This mixture was mixed with an equal volume of 1×10^5 cloned iHepSCs suspended in cholangiocytic differentiation medium (CDM) (DMEM/F12 medium supplemented with 10% fetal bovine serum [HyClone], 20 ng/ml HGF [BD]). The cell suspension was transferred into a 6-well plate and left at 37°C for 30 min. After the gel formed, the CDM was gently added on to the gel.

Assay for Transport of Fluorescent Dye

iHepSCs were cultured in a chambered coverslip (Nalgene Nunc) to form cysts in a 3D system consisting of 1.2 mg/ml collagen type 1 and 40% Matrigel for 7 days. The method to assess the transport of rhodamine 123 and inhibition effect of R-(+)-verapamil was performed same as described previously in Tanimizu et al. (2007).

Mice Breeding and Cell Transplantation

Fah$^{-/-}$ mice, Nod/SCID mice, and 129S4 mice were maintained according to institutional guidelines. Fah$^{-/-}$ mice (8–10 weeks old) were maintained with 7.5 mg/l NTBC in the drinking water. For cell transplantation, 1×10^6 iHepSCs were injected intrasplenically into the Fah$^{-/-}$ mice without NTBC. They were sacrificed at 8 weeks after cell transplantation; the recipient livers were harvested and were fixed in 4% phosphate-buffered paraformaldehyde overnight at 4°C. Five random serial sections from left, middle, and right liver lobes were examined by IHC analysis to determine the donor cell repopulation.

DDC-treated mice were put on a diet containing 0.1% DDC (wt/wt) as previously described (Wang et al., 2003b). Three days after DDC diet treatment, the mice were transplanted intrasplenically with 1×10^6 iHepSCs labeled

with eGFP or LacZ by lentivirus and were kept on DDC diet. Mice recipients were sacrificed 3 weeks after cell transplantation. Liver cryostat sections (10 μm) were observed under a fluorescence microscope to detect the eGFP-positive transplanted cells and were examined with anti-CK19 antibody, anti-CK7 antibody, anti-EpCAM antibody, and anti-Ostα antibody by IHC for cholangiocyte markers.

ACCESSION NUMBERS

The GEO accession number for the microarray data reported in this paper is GSE48486.

SUPPLEMENTAL INFORMATION

Supplemental Information for this article Supplemental Experimental Procedures, four figures, and two tables and can be found with this article online at http://dx.doi.org/10.1016/j.stem.2013.06.017.

REFERENCES

Ballatori, N., Christian, W.V., Lee, J.Y., Dawson, P.A., Soroka, C.J., Boyer, J.L., Madejczyk, M.S., and Li, N. (2005). OSTalpha-OSTbeta: a major basolateral bile acid and steroid transporter in human intestinal, renal, and biliary epithelia. Hepatology 42, 1270–1279.

Caiazzo, M., Dell'Anno, M.T., Dvoretskova, E., Lazarevic, D., Taverna, S., Leo, D., Sotnikova, T.D., Menegon, A., Roncaglia, P., Colciago, G., et al. (2011). Direct generation of functional dopaminergic neurons from mouse and human fibroblasts. Nature 476, 224–227.

Coffinier, C., Gresh, L., Fiette, L., Tronche, F., Schütz, G., Babinet, C., Pontoglio, M., Yaniv, M., and Barra, J. (2002). Bile system morphogenesis defects and liver dysfunction upon targeted deletion of HNF1beta. Development 129, 1829–1838.

Davis, R.L., Weintraub, H., and Lassar, A.B. (1987). Expression of a single transfected cDNA converts fibroblasts to myoblasts. Cell 51, 987–1000.

Dorrell, C., Erker, L., Schug, J., Kopp, J.L., Canaday, P.S., Fox, A.J., Smirnova, O., Duncan, A.W., Finegold, M.J., Sander, M., et al. (2011). Prospective isolation of a bipotential clonogenic liver progenitor cell in adult mice. Genes Dev. 25, 1193–1203.

Efe, J.A., Hilcove, S., Kim, J., Zhou, H., Ouyang, K., Wang, G., Chen, J., and Ding, S. (2011). Conversion of mouse fibroblasts into cardiomyocytes using a direct reprogramming strategy. Nat. Cell Biol. 13, 215–222.

Feng, R., Desbordes, S.C., Xie, H., Tillo, E.S., Pixley, F., Stanley, E.R., and Graf, T. (2008). PU.1 and C/EBPalpha/beta convert fibroblasts into macrophage-like cells. Proc. Natl. Acad. Sci. USA *105*, 6057–6062.

Furuyama, K., Kawaguchi, Y., Akiyama, H., Horiguchi, M., Kodama, S., Kuhara, T., Hosokawa, S., Elbahrawy, A., Soeda, T., Koizumi, M., et al. (2011). Continuous cell supply from a Sox9-expressing progenitor zone in adult liver, exocrine pancreas and intestine. Nat. Genet. *43*, 34–41.

Grompe, M., al-Dhalimy, M., Finegold, M., Ou, C.N., Burlingame, T., Kennaway, N.G., and Soriano, P. (1993). Loss of fumarylacetoacetate hydrolase is responsible for the neonatal hepatic dysfunction phenotype of lethal albino mice. Genes Dev. *7*(12A), 2298–2307.

Han, D.W., Tapia, N., Hermann, A., Hemmer, K., Höing, S., Araúzo-Bravo, M.J., Zaehres, H., Wu, G., Frank, S., Moritz, S., et al. (2012). Direct reprogramming of fibroblasts into neural stem cells by defined factors. Cell Stem Cell *10*, 465–472.

He, Z., Zhang, H., Zhang, X., Xie, D., Chen, Y., Wangensteen, K.J., Ekker, S.C., Firpo, M., Liu, C., Xiang, D., et al. (2010). Liver xeno-repopulation with human hepatocytes in Fah-/-Rag2-/- mice after pharmacological immunosuppression. Am. J. Pathol. *177*, 1311–1319.

He, Z.Y., Deng, L., Li, Y.F., Xiang, D., Hu, J.K., Chen, Y.X., Wang, M.J., Chen, F., Liu, C.C., Li, W.L., et al. (2012). Murine embryonic stem cell-derived hepatocytes correct metabolic liver disease after serial liver repopulation. Int. J. Biochem. Cell Biol. *44*, 648–658.

Huang, P., He, Z., Ji, S., Sun, H., Xiang, D., Liu, C., Hu, Y., Wang, X., and Hui, L. (2011). Induction of functional hepatocyte-like cells from mouse fibroblasts by defined factors. Nature *475*, 386–389.

Huch, M., Dorrell, C., Boj, S.F., van Es, J.H., Li, V.S., van de Wetering, M., Sato, T., Hamer, K., Sasaki, N., Finegold, M.J., et al. (2013). In vitro expansion of single Lgr5+ liver stem cells induced by Wnt-driven regeneration. Nature *494*, 247–250.

Ieda, M., Fu, J.D., Delgado-Olguin, P., Vedantham, V., Hayashi, Y., Bruneau, B.G., and Srivastava, D. (2010). Direct reprogramming of fibroblasts into functional cardiomyocytes by defined factors. Cell *142*, 375–386.

Ishikawa, T., Factor, V.M., Marquardt, J.U., Raggi, C., Seo, D., Kitade, M., Conner, E.A., and Thorgeirsson, S.S. (2012). Hepatocyte growth factor/c-met signaling is required for stem-cell-mediated liver regeneration in mice. Hepatology *55*, 1215–1226.

Jakubowski, A., Ambrose, C., Parr, M., Lincecum, J.M., Wang, M.Z., Zheng, T.S., Browning, B., Michaelson, J.S., Baetscher, M., Wang, B., et al. (2005). TWEAK induces liver progenitor cell proliferation. J. Clin. Invest. *115*, 2330–2340.

Kim, J., Efe, J.A., Zhu, S., Talantova, M., Yuan, X., Wang, S., Lipton, S.A., Zhang, K., and Ding, S. (2011). Direct reprogramming of mouse fibroblasts to neural progenitors. Proc. Natl. Acad. Sci. USA *108*, 7838–7843.

Laiosa, C.V., Stadtfeld, M., Xie, H., de Andres-Aguayo, L., and Graf, T. (2006). Reprogramming of committed T cell progenitors to macrophages and dendritic cells by C/EBP alpha and PU.1 transcription factors. Immunity *25*, 731–744.

Le Lay, J., and Kaestner, K.H. (2010). The Fox genes in the liver: from organogenesis to functional integration. Physiol. Rev. *90*, 1–22.

Li, W.L., Su, J., Yao, Y.C., Tao, X.R., Yan, Y.B., Yu, H.Y., Wang, X.M., Li, J.X., Yang, Y.J., Lau, J.T., and Hu, Y.P. (2006). Isolation and characterization of bipotent liver progenitor cells from adult mouse. Stem Cells *24*, 322–332.

Li, F., Liu, P., Liu, C., Xiang, D., Deng, L., Li, W., Wangensteen, K., Song, J., Ma, Y., Hui, L., et al. (2010). Hepatoblast-like progenitor cells derived from embryonic stem cells can repopulate livers of mice. Gastroenterology *139*, 2158–2169, e8.

Liu, X., Li, F., Stubblefield, E.A., Blanchard, B., Richards, T.L., Larson, G.A., He, Y., Huang, Q., Tan, A.C., Zhang, D., et al. (2012). Direct reprogramming of human fibroblasts into dopaminergic neuron-like cells. Cell Res. *22*, 321–332.

Lokmane, L., Haumaitre, C., Garcia-Villalba, P., Anselme, I., Schneider-Maunoury, S., and Cereghini, S. (2008). Crucial role of vHNF1 in vertebrate hepatic specification. Development *135*, 2777–2786.

Lujan, E., Chanda, S., Ahlenius, H., Südhof, T.C., and Wernig, M. (2012). Direct conversion of mouse fibroblasts to self-renewing, tripotent neural precursor cells. Proc. Natl. Acad. Sci. USA *109*, 2527–2532.

Moritoki, Y., Ueno, Y., Kanno, N., Yamagiwa, Y., Fukushima, K., Gershwin, M.E., and Shimosegawa, T. (2006). Lack of evidence that bone marrow cells contribute to cholangiocyte repopulation during experimental cholestatic ductal hyperplasia. Liver Int. *26*, 457–466.

Nejak-Bowen, K., and Monga, S.P. (2008). Wnt/beta-catenin signaling in hepatic organogenesis. Organogenesis *4*, 92–99.

Oertel, M., Menthena, A., Chen, Y.Q., Teisner, B., Jensen, C.H., and Shafritz, D.A. (2008). Purification of fetal liver stem/progenitor cells containing all the repopulation potential for normal adult rat liver. Gastroenterology *134*, 823–832.

Okabe, M., Tsukahara, Y., Tanaka, M., Suzuki, K., Saito, S., Kamiya, Y., Tsujimura, T., Nakamura, K., and Miyajima, A. (2009). Potential hepatic stem cells reside in EpCAM+ cells of normal and injured mouse liver. Development *136*, 1951–1960.

Overturf, K., Al-Dhalimy, M., Tanguay, R., Brantly, M., Ou, C.N., Finegold, M., and Grompe, M. (1996). Hepatocytes corrected by gene therapy are selected in vivo in a murine model of hereditary tyrosinaemia type I. Nat. Genet. *12*, 266–273.

Pang, Z.P., Yang, N., Vierbuchen, T., Ostermeier, A., Fuentes, D.R., Yang, T.Q., Citri, A., Sebastiano, V., Marro, S., Südhof, T.C., and Wernig, M. (2011). Induction of human neuronal cells by defined transcription factors. Nature *476*, 220–223.

Park, I.H., Zhao, R., West, J.A., Yabuuchi, A., Huo, H., Ince, T.A., Lerou, P.H., Lensch, M.W., and Daley, G.Q. (2008). Reprogramming of human somatic cells to pluripotency with defined factors. Nature *451*, 141–146.

Pfisterer, U., Kirkeby, A., Torper, O., Wood, J., Nelander, J., Dufour, A., Björklund, A., Lindvall, O., Jakobsson, J., and Parmar, M. (2011). Direct conversion of human fibroblasts to dopaminergic neurons. Proc. Natl. Acad. Sci. USA *108*, 10343–10348.

Preisegger, K.H., Factor, V.M., Fuchsbichler, A., Stumptner, C., Denk, H., and Thorgeirsson, S.S. (1999). Atypical ductular proliferation and its inhibition by transforming growth factor beta1 in the 3,5-diethoxycarbonyl-1,4-dihydrocollidine mouse model for chronic alcoholic liver disease. Lab. Invest. *79*, 103–109.

Ring, K.L., Tong, L.M., Balestra, M.E., Javier, R., Andrews-Zwilling, Y., Li, G., Walker, D., Zhang, W.R., Kreitzer, A.C., and Huang, Y. (2012). Direct reprogramming of mouse and human fibroblasts into multipotent neural stem cells with a single factor. Cell Stem Cell *11*, 100–109.

Sackett, S.D., Li, Z., Hurtt, R., Gao, Y., Wells, R.G., Brondell, K., Kaestner, K.H., and Greenbaum, L.E. (2009). Foxl1 is a marker of bipotential hepatic progenitor cells in mice. Hepatology *49*, 920–929.

Sekiya, S., and Suzuki, A. (2011). Direct conversion of mouse fibroblasts to hepatocyte-like cells by defined factors. Nature *475*, 390–393.

Shafritz, D.A., and Dabeva, M.D. (2002). Liver stem/progenitor cells and their transplantation: from fantasy to reality as we enter the new millennium. EJBM *19*, 20–32.

Shin, S., Walton, G., Aoki, R., Brondell, K., Schug, J., Fox, A., Smirnova, O., Dorrell, C., Erker, L., Chu, A.S., et al. (2011). Foxl1-Cre-marked adult hepatic progenitors have clonogenic and bilineage differentiation potential. Genes Dev. *25*, 1185–1192.

Son, E.Y., Ichida, J.K., Wainger, B.J., Toma, J.S., Rafuse, V.F., Woolf, C.J., and Eggan, K. (2011). Conversion of mouse and human fibroblasts into functional spinal motor neurons. Cell Stem Cell *9*, 205–218.

Szabo, E., Rampalli, S., Risueño, R.M., Schnerch, A., Mitchell, R., Fiebig-Comyn, A., Levadoux-Martin, M., and Bhatia, M. (2010). Direct conversion of human fibroblasts to multilineage blood progenitors. Nature *468*, 521–526.

Takahashi, K., and Yamanaka, S. (2006). Induction of pluripotent stem cells from mouse embryonic and adult fibroblast cultures by defined factors. Cell *126*, 663–676.

Tanimizu, N., Saito, H., Mostov, K., and Miyajima, A. (2004). Long-term culture of hepatic progenitors derived from mouse Dlk+ hepatoblasts. J. Cell Sci. *117*, 6425–6434.

Tanimizu, N., Miyajima, A., and Mostov, K.E. (2007). Liver progenitor cells develop cholangiocyte-type epithelial polarity in three-dimensional culture. Mol. Biol. Cell *18*, 1472–1479.

Thier, M., Wörsdörfer, P., Lakes, Y.B., Gorris, R., Herms, S., Opitz, T., Seiferling, D., Quandel, T., Hoffmann, P., Nöthen, M.M., et al. (2012). Direct conversion of fibroblasts into stably expandable neural stem cells. Cell Stem Cell 10, 473–479.

Thompson, M.D., Awuah, P., Singh, S., and Monga, S.P. (2010). Disparate cellular basis of improved liver repair in beta-catenin-overexpressing mice after long-term exposure to 3,5-diethoxycarbonyl-1,4-dihydrocollidine. Am. J. Pathol. 177, 1812–1822.

Vierbuchen, T., Ostermeier, A., Pang, Z.P., Kokubu, Y., Südhof, T.C., and Wernig, M. (2010). Direct conversion of fibroblasts to functional neurons by defined factors. Nature 463, 1035–1041.

Wang, X., Willenbring, H., Akkari, Y., Torimaru, Y., Foster, M., Al-Dhalimy, M., Lagasse, E., Finegold, M., Olson, S., and Grompe, M. (2003a). Cell fusion is the principal source of bone-marrow-derived hepatocytes. Nature 422, 897–901.

Wang, X., Foster, M., Al-Dhalimy, M., Lagasse, E., Finegold, M., and Grompe, M. (2003b). The origin and liver repopulating capacity of murine oval cells. Proc. Natl. Acad. Sci. USA 100(Suppl 1), 11881–11888.

Zaret, K.S. (2008). Genetic programming of liver and pancreas progenitors: lessons for stem-cell differentiation. Nat. Rev. Genet. 9, 329–340.

Zaret, K.S., and Grompe, M. (2008). Generation and regeneration of cells of the liver and pancreas. Science 322, 1490–1494.